ACS Catalysis

Letter

pubs.acs.org/acscatalysis

Mechanistic Insights into Ruthenium-Catalyzed Production of H_2 and CO_2 from Methanol and Water: A DFT Study

Xinzheng Yang*

Beijing National Laboratory for Molecular Sciences, State Key Laboratory for Structural Chemistry of Unstable and Stable Species, Institute of Chemistry, Chinese Academy of Sciences, Beijing 100190, P. R. China

Supporting Information

ABSTRACT: A density functional theory study of the reaction mechanism of the production of H_2 and CO_2 from methanol and water catalyzed by an aliphatic PNP pincer ruthenium complex, (PNP)Ru(H)CO, reveals three interrelated catalytic cycles for the release of three H_2 molecules: the dehydrogenation of methanol to formaldehyde, the coupling of formaldehyde and hydroxide for the formation of formic acid, and the dehydrogenation of formic acid. The formation of all three H_2 molecules undergoes the same self-promoted mechanism that features a methanol or a water molecule acting as a bridge for the transfer of a ligand proton to the metal hydride in a key intermediate, *trans*-(*H*PNP)Ru(H)$_2$CO.

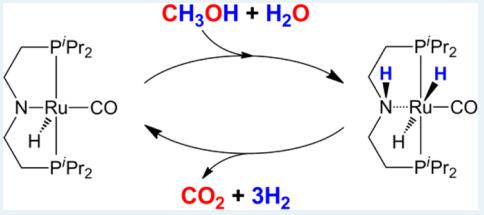

KEYWORDS: *catalytic mechanism, dehydrogenation, methanol, water, carbon dioxide, ruthenium*

Although the conception of "hydrogen-economy" emerged over 40 years ago, the efficiency and cost of hydrogen production and storage are still the primary bottlenecks in the practical application of hydrogen as a clean and renewable energy carrier. Compared to other hydrogen storage material candidates, methanol contains 12.6 wt % of hydrogen and is a liquid at room temperature, which allows it to be efficiently transported using the existing petroleum pipeline system at a very low extra cost. In addition, methanol could be produced from low-cost biomass at large-scale, which provides a potential solution for a sustainable solar-hydrogen energy conversion.[1] Therefore, with the advocacy of the development of "methanol-economy" by Olah and his colleges,[2] the utilization of methanol as an alternative fuel and hydrogen carrier has attracted increasing attention in recent years.[3] Although steady progress in catalytic dehydrogenation of methanol has been achieved in recent years,[4] most of the reported catalysts have rather low efficiencies and can only release one H_2 molecule from each methanol molecule with the generation of carbon-containing byproducts. The efficiency of current state-of-the-art platinum-based methanol fuel cells is limited to about 40% because of the high operating temperature (>200 °C).[5]

An ideal way to use methanol as a hydrogen carrier is the conversion of a methanol−water mixture into CO_2 and H_2, which means the entire hydrogen content (12 wt %) is used (eq 1)

$$CH_3OH + H_2O \rightarrow CO_2 + 3H_2 \quad (1)$$

One of the most recent advances in this area is a ruthenium catalytic system developed by Beller and co-workers.[6] Using an aliphatic PNP pincer ruthenium complex (*H*PNP)Ru(H)(Cl)-CO {*H*PNP = bis[2-(diisopropylphosphino)-ethyl]amine} as the catalyst precursor and strongly basic conditions for the generation of the active catalyst, (PNP)Ru(H)CO (**1**), they have achieved a turnover frequency (TOF) of 4700 h^{-1} and a turnover number (TON) of 350 000 for the dehydrogenation of methanol under mild conditions (<100 °C). Almost at the same time, Rodríguez-Lugo et al.[7] developed a ruthenium complex with a chelating bis(olefin) diazadiene ligand, [K(dme)$_2$][RuH(trop$_2$dad)], which could catalyze the conversion of a methanol−water mixture selectively to CO_2 and H_2 gases under neutral conditions. The trop$_2$dad ligand is also a chemically "noninnocent" ligand and cooperates with ruthenium for dehydrogenation of methanol and water.

Although the above findings are great breakthroughs in "methanol−hydrogen economy", a major obstacle for their practical use is the nobility of Ru. The design of low-cost and environmentally benign base metal catalysts for efficient and sustainable production of hydrogen from methanol are still highly attractive and challenging.[8] Beller and co-workers have recently developed an aliphatic PNP pincer iron complex for the catalytic dehydrogenation of aqueous methanol, but the TOF and TON are up to 777 h^{-1} and 10 000, respectively, much lower than the Ru catalysts.[9] The understanding of the mechanistic insights into the dehydrogenation of methanol catalyzed by the Ru complexes would greatly benefit the design of non-noble metal catalysts.

In this Letter, we report a density functional theory (DFT) study of the reaction mechanism for the production of three H_2 molecules and one CO_2 molecule from methanol and water catalyzed by **1**. Three interrelated catalytic cycles for the dehydrogenation of methanol to formaldehyde, the coupling of formaldehyde and hydroxide to formic acid, and the dehydrogenation of formic acid to CO_2 are proposed with

Received: January 16, 2014
Revised: February 27, 2014
Published: February 28, 2014

   dx.doi.org/10.1021/cs500061u | ACS Catal. 2014, 4, 1129−1133

the analyses of detailed energy profile and key structures. All DFT calculations in this study were performed using the Gaussian 09 suite of ab initio programs[10] for the M06 functional[11] in conjugation with the all-electron 6-31++G(d,p) basis set for H, C, N, O, and P,[12] and the Stuttgart relativistic effective core potential basis set for Ru (ECP28MWB).[13] Other computational details are provided in the Supporting Information. Unless otherwise noted, the energies reported in this paper are Gibbs free energies with solvent effect corrections for methanol.

As shown in Scheme 1 and the corresponding energy profile (Figure 1), the reaction begins with a quick transfer of the hydroxyl proton in a methanol molecule to the ligand nitrogen in **1** for the formation of a slightly more stable intermediate **2**. The O–H bond cleavage barrier is only 1.2 kcal/mol ($TS_{1,2}$, Figure 2). Then, a C–H bond in methoxy splits easily and transfers a hydride to the metal center through transition state $TS_{2,3}$ (Figure 2) for the formation of formaldehyde. $TS_{2,3}$ is only 10.5 kcal/mol higher than **2**. The formaldehyde molecule dissociates from **3** and forms a slightly more stable H_2COOH^- anion with the hydroxide anion, which could be the base in the solvent or generated from the cleavage of water (Scheme 2, Figure 3). The dihydride complex, *trans*-(*H*PNP)Ru(H)$_2$CO (**4**), is 1.2 kcal/mol more stable than **1**.

Scheme 1. Catalytic Cycle for the Dehydrogenation of Methanol with Direct Proton Transfer (Red) and Relayed Proton Transfer (Blue) Pathways for the Formation of the First H_2 Molecule

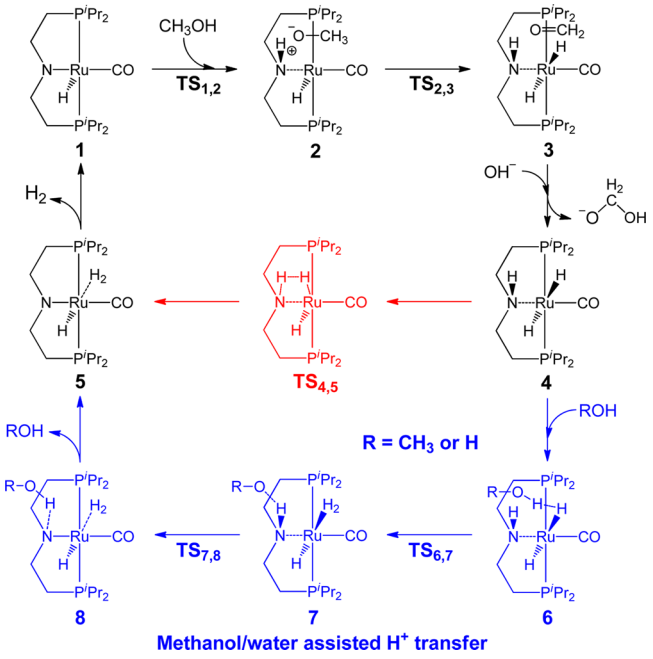

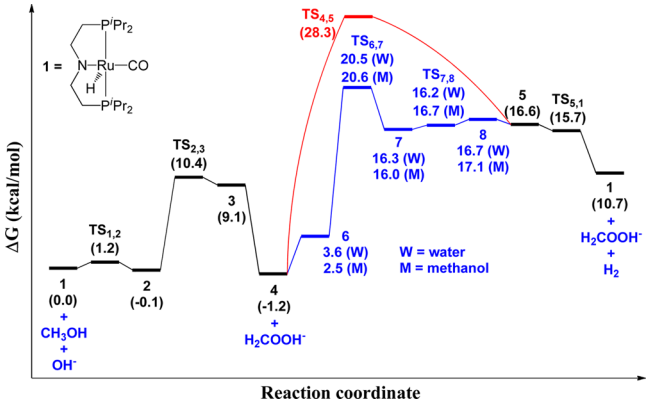

Figure 1. Free energy profile of the catalytic cycle shown in Scheme 1 for the dehydrogenation of methanol with the release of the first H_2 molecule.

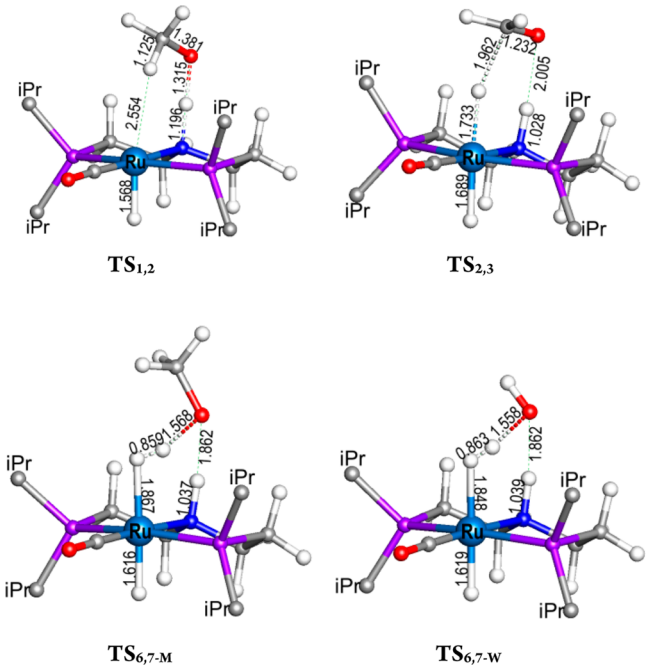

Figure 2. Optimized structures of transition states $TS_{1,2}$ (1195*i* cm^{-1}), $TS_{2,3}$ (32*i* cm^{-1}), $TS_{6,7\text{-M}}$ (452*i* cm^{-1}), and $TS_{6,7\text{-W}}$ (571*i* cm^{-1}). Isopropyl groups are omitted for clarity. Bond lengths are in Å.

Scheme 2. Catalytic Cycle for the Cleavage of H_2O and the Formation of Formic Acid and the Second H_2

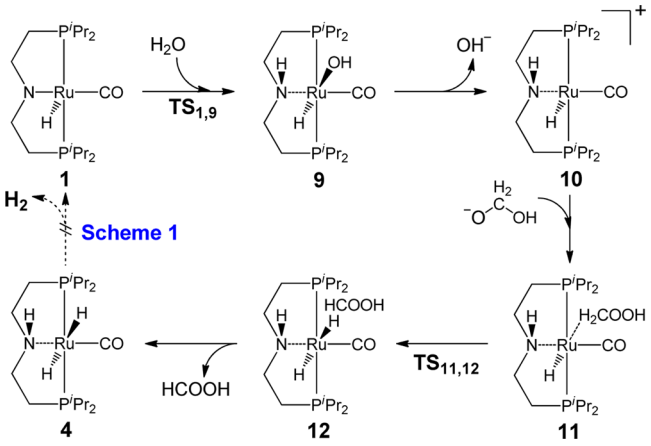

In order to release H_2 and regenerate the catalyst, the formation of a dihydrogen complex **5** is required. Starting from **4**, there are three ways to form **5**. The most straightforward one is the direct transfer of a proton from the ligand nitrogen to the metal hydride through transition state $TS_{4,5}$. However, the calculated free energy barrier of this direct proton transfer is

dx.doi.org/10.1021/cs500061u | ACS Catal. 2014, 4, 1129–1133

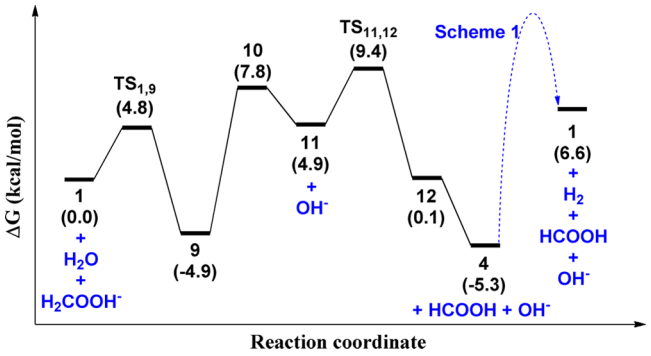

Figure 3. Free energy profile of the catalytic cycle shown in Scheme 2 for the cleavage of H_2O and the formation of formic acid, as well as the release of the second H_2 molecule.

29.5 kcal/mol (**4** → $\mathbf{TS}_{4,5}$), which is too high to account for the observed reaction rate under mild condition. Instead of direct proton transfer, we found that an extra water or methanol molecule can act as a proton transfer tunnel and assist the formation of H_2. In this reaction pathway, a water or methanol molecule approaches **4** and forms a slightly less stable intermediate $\mathbf{6}_W$ or $\mathbf{6}_M$ with a strong intermolecular Ru−$H^{\delta-}\cdots H^{\delta+}$−O dihydrogen bond. The $H^{\delta-}\cdots H^{\delta+}$ distances in the dihydrogen bonds in $\mathbf{6}_M$ and $\mathbf{6}_W$ are 1.657 and 1.686 Å, respectively, which are similar to the dihydrogen bond length found in our recent theoretical study of the catalytic dehydrogenation of ethanol[14] and shorter than the H···H distances in a range of 1.7 − 2.2 Å in most M−$H^{\delta-}\cdots H^{\delta+}$−X dihydrogen bonds reported so far.[15]

After the formation of $\mathbf{6}_W$ or $\mathbf{6}_M$, the hydroxyl proton in water or methanol transfers to the metal hydride through transition state $\mathbf{TS}_{6,7\text{-}W}$ or $\mathbf{TS}_{6,7\text{-}M}$ for the formation of H_2 in intermediate $\mathbf{7}_W$ or $\mathbf{7}_M$. $\mathbf{TS}_{6,7\text{-}W}$ and $\mathbf{TS}_{6,7\text{-}M}$ are near 8 kcal/mol lower than $\mathbf{TS}_{4,5}$, and they are only 21.8 and 21.7 kcal/mol higher than **4**, respectively. The hydroxyl group in $\mathbf{7}_W$ or the methoxy group in $\mathbf{7}_M$ can easily take a proton from the ligand nitrogen and reform a water or methanol molecule through transition state $\mathbf{TS}_{7,8\text{-}W}$ or $\mathbf{TS}_{7,8\text{-}M}$. The release of the reformed water or methanol molecule from $\mathbf{8}_W$ or $\mathbf{8}_M$ and the formation of **5** is 0.1 or 0.5 kcal/mol downhill, respectively. The release of H_2 from **5** for the regeneration of **1** is 5.9 kcal/mol downhill. After comparing all relative energies of the catalytic cycle shown in Figure 1, we can conclude that the formation of H_2 through the proton transfer relayed by a water molecule ($\mathbf{TS}_{6,7\text{-}W}$) is the rate-determining step with a total energy barrier of 21.7 kcal/mol (**4** → $\mathbf{TS}_{6,7\text{-}W}$). The formation of H_2 through the proton transfer relayed by methanol is highly competitive with a barrier of 21.8 kcal/mol, which is only 0.1 kcal/mol higher than $\mathbf{TS}_{6,7\text{-}W}$.

Simultaneous to the dehydrogenation of methanol and the formation of formaldehyde, a water molecule also fills the vacant position in **1** and splits quickly through $\mathbf{TS}_{1,9}$ (Figure 4). Then the hydroxyl anion in **9** can easily exchange with the H_2COOH^- anion formed in the dehydrogenation of methanol and forms intermediate **11**, which is 9.8 kcal/mol less stable than **9** in free energy. Then, a formic acid molecule is formed through the cleavage of a C−H bond for the transfer of a methylene hydride in the H_2COOH^- anion to Ru ($\mathbf{TS}_{11,12}$, Figure 4). The dissociation of formic acid from **12** and the formation of **4** is 5.4 kcal/mol downhill. Then the second H_2 molecule can be formed and released from **4** through the water

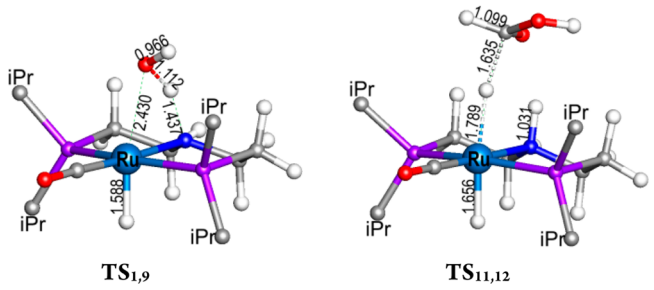

Figure 4. Optimized structures of $\mathbf{TS}_{1,9}$ (439*i* cm^{-1}) and $\mathbf{TS}_{11,12}$ (648*i* cm^{-1}). Bond lengths are in Å.

or methanol relayed proton transfer pathways shown in Scheme 1. Because the hydroxide anion keeps reacting with the formaldehyde generated from dehydrogenation of methanol for the formation of H_2COOH^-, the basicity of the solvent remains constant after the initial stage of the reaction.

As shown in Scheme 3 and Figure 5, once a formic acid molecule is formed, it reacts immediately with **1** and forms a

Scheme 3. Catalytic Cycle for the Dehydrogenation of Formic Acid for the Formation of CO_2 and the Third H_2

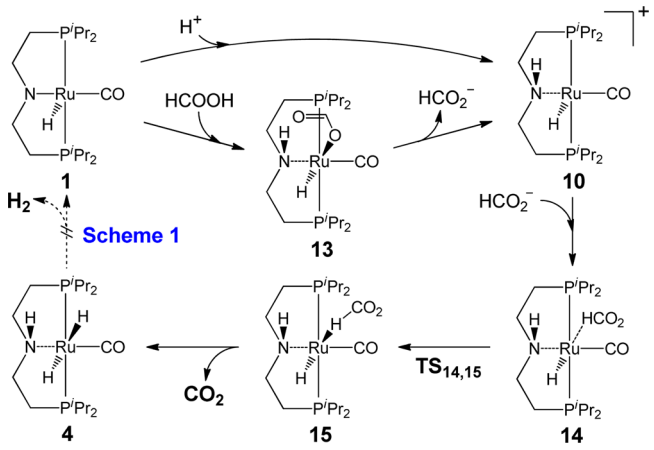

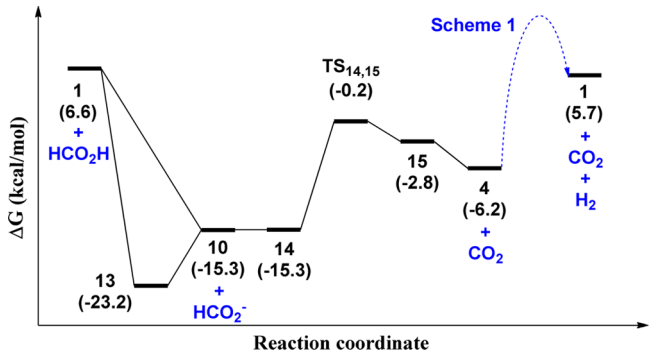

Figure 5. Free energy profile of the catalytic cycle shown in Scheme 3 for the dehydrogenation of formic acid.

29.8 kcal/mol more stable intermediate **13** (Figure 6). Because of the acidity of formic acid, we were unable to locate a transition state for the cleavage of the O−H bond in formic acid when it approaches **1**. The acidity of formic acid could also lead the direct formation of **10** from **1** through the protonation of ligand nitrogen. The rearrangement of the formate group in **13** or the approaching of the solvent formate to **10** could form

dx.doi.org/10.1021/cs500061u | ACS Catal. 2014, 4, 1129−1133

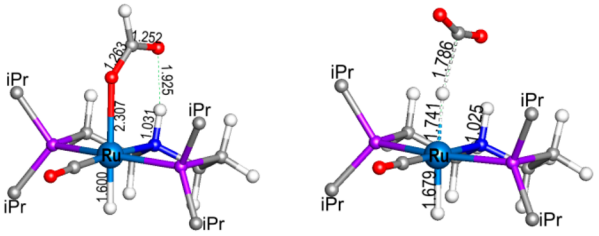

13 $TS_{14,15}$

Figure 6. Optimized structures of **13** and $TS_{14,15}$ (607*i* cm^{-1}). Bond lengths are in Å.

an unstable intermediate **14**, in which a formate group binds to **10** through very weak Ru···H−C and N−H···O interactions. Then the formate hydride in **14** is transferred directly from carbon to ruthenium through transition state $TS_{14,15}$ (Figure 6), which is 23.0 kcal/mol higher than **13**. The release of CO_2 from **15** and the generation of **4** is 3.4 kcal/mol downhill. With the formation and release of the third H_2 molecule in the newly generated **4**, a complete catalytic mechanism for the production of hydrogen and carbon dioxide from methanol and water has been established.

In summary, we have conducted a density functional theory study of the production of hydrogen and carbon dioxide from methanol and water catalyzed by **1**. Our computational study reveals three interrelated catalytic cycles: dehydrogenation of methanol to formaldehyde, coupling of formaldehyde and hydroxide for the formation of formic acid, and dehydrogenation of formic acid. The overall mechanism and the relationships of those reaction pathways are summarized in Scheme 4. Each catalytic cycle produces a H_2 molecule through

Scheme 4. Overall Mechanism for the Production of Three H_2 and One CO_2 from Methanol and Water

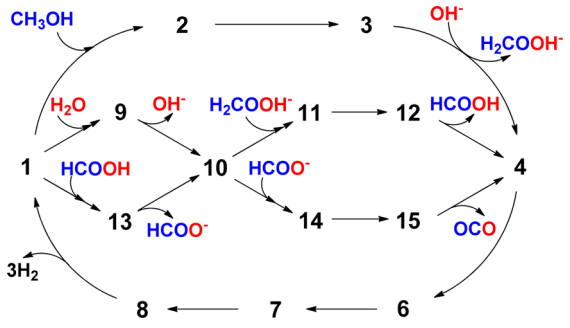

a self-promoted mechanism that features an extra methanol or water molecule acting as a bridge for the transfer of a proton from the ligand nitrogen to the metal hydride in **4**. The calculated total free energy barriers of above three catalytic cycles are 21.7, 14.3, and 23.0 kcal/mol, respectively, which are consistent with the observed catalytic efficiency at less than 100 °C. We believe the production of hydrogen and carbon dioxide from methanol and water promoted by an aliphatic PNP pincer iron complex, (PNP)Fe(H)CO,[9,14] undergoes a similar catalytic mechanism with slightly higher energy barriers. Our mechanism explains the essential role of the noninnocent aliphatic PNP ligand in the catalytic reaction and points the way to finding new catalysts with lower cost and higher efficiency, as the hydrogen-facilitated proton transfer from an ancillary ligand may be essential for low energy hydrogen transfers.

■ ASSOCIATED CONTENT

Supporting Information

Computational details, solvent corrected absolute free energies, and atomic coordinates of all optimized structures. This material is available free of charge via the Internet at http://pubs.acs.org.

■ AUTHOR INFORMATION

Corresponding Author

*E-mail: xyang@iccas.ac.cn.

Notes

The authors declare no competing financial interest.

■ ACKNOWLEDGMENTS

This work is supported by the 100-Talent Program of Chinese Academy of Sciences, the "One-Three-Five" Strategic Planning of Institute of Chemistry, Chinese Academy of Sciences (CMS-PY-201305), and the National Natural Science Foundation of China (21373228). Part of the computational work was performed in the Molecular Graphics and Computation Facility (MGCF) in the College of Chemistry at University of California (Berkeley, CA). MGCF is supported by the U.S. National Science Foundation (CHE-0840505). I acknowledge the support of Dr. Kathleen A. Durkin.

■ REFERENCES

(1) Navarro, R. M.; Peña, M. A.; Fierro, J. L. G. *Chem. Rev.* **2007**, *107*, 3952−3991.
(2) Olah, G. A.; Prakash, G.; Goeppert, A. *Chem. Eng. News* **2003**, *81*, 5.
(3) Palo, D. R.; Dagle, R. A.; Holladay, J. D. *Chem. Rev.* **2007**, *107*, 3992−4021.
(4) (a) Shinoda, S.; Itagaki, H.; Saito, Y. *Chem. Commun.* **1985**, 860−861. (b) Makita, K.; Nomura, K.; Saito, Y. *J. Mol. Catal.* **1994**, *89*, 143−150. (c) Okamoto, Y.; Ida, S.; Hyodo, J.; Hagiwara, H.; Ishihara, T. *J. Am. Chem. Soc.* **2011**, *133*, 18034−18037. (d) Gärtner, F.; Losse, S.; Boddien, A.; Pohl, M.-M.; Denurra, S.; Junge, H.; Beller, M. *ChemSusChem* **2012**, *5*, 530−533. (e) Johnson, T. C.; Morris, D. J.; Wills, R. *Chem. Soc. Rev.* **2010**, *39*, 81−88.
(5) (a) Cortright, R. D.; Davda, R. R.; Dumesic, J. A. *Nature* **2002**, *418*, 964−967. (b) Shabaker, J. W.; Davda, R. R.; Huber, G. W.; Cortright, R. D.; Dumesic, J. A. *J. Catal.* **2003**, *215*, 344−352.
(6) (a) Nielsen, M.; Alberico, E.; Baumann, W.; Drexler, H.-J.; Junge, H.; Gladiali, S.; Beller, M. *Nature* **2013**, *495*, 85−89. (b) Stephan, D. W. *Nature* **2013**, *495*, 54−55.
(7) Rodríguez-Lugo, R. E.; Trincado, M.; Vogt, M.; Tewes, F.; Santiso-Quinones, G.; Grützmacher, H. *Nat. Chem.* **2013**, *5*, 342−347.
(8) *Catalysis Without Precious Metals*; Bullock, R. M., Ed.; Wiley-VCH: Weinheim, Germany, 2010.
(9) Alberico, E.; Sponholz, P.; Cordes, C.; Nielsen, M.; Drexler, H.-J.; Baumann, W.; Junge, H.; Beller, M. *Angew. Chem., Int. Ed.* **2013**, *52*, 14162−14166.
(10) Frisch, M. J.; Trucks, G. W.; Schlegel, H. B.; Scuseria, G. E.; Robb, M. A.; Cheeseman, J. R.; Scalmani, G.; Barone, V.; Mennucci, B.; Petersson, G. A.; Nakatsuji, H.; Caricato, M.; Li, X.; Hratchian, H. P.; Izmaylov, A. F.; Bloino, J.; Zheng, G.; Sonnenberg, J. L.; Hada, M.; Ehara, M.; Toyota, K.; Fukuda, R.; Hasegawa, J.; Ishida, M.; Nakajima, T.; Honda, Y.; Kitao, O.; Nakai, H.; Vreven, T.; Montgomery, Jr., J. A.; Peralta, J. E.; Ogliaro, F.; Bearpark, M.; Heyd, J. J.; Brothers, E.; Kudin, K. N.; Staroverov, V. N.; Kobayashi, R.; Normand, J.; Raghavachari, K.; Rendell, A.; Burant, J. C.; Iyengar, S. S.; Tomasi, J.; Cossi, M.; Rega, N.; Millam, N. J.; Klene, M.; Knox, J. E.; Cross, J. B.; Bakken, V.; Adamo, C.; Jaramillo, J.; Gomperts, R.; Stratmann, R. E.; Yazyev, O.; Austin, A. J.; Cammi, R.; Pomelli, C.; Ochterski, J. W.; Martin, R. L.; Morokuma, K.; Zakrzewski, V. G.; Voth, G. A.; Salvador, P.; Dannenberg, J. J.; Dapprich, S.; Daniels, A. D.; Farkas, Ö.;

Foresman, J. B.; Ortiz, J. V.; Cioslowski, J.; Fox, D. J. *Gaussian 09*, revision C.01; Gaussian, Inc.: Wallingford, CT, 2010.
(11) Zhao, Y.; Truhlar, D. G. *J. Chem. Phys.* **2006**, *125*, 194101.
(12) (a) Hehre, W. J.; Ditchfield, R.; Pople, J. A. *J. Chem. Phys.* **1972**, *56*, 2257−2261. (b) Hariharan, P. C.; Pople, J. A. *Theor. Chim. Acta* **1973**, *28*, 213−222. (c) Krishnan, R.; Binkley, J. S.; Seeger, R.; Pople, J. A. *J. Chem. Phys.* **1980**, *72*, 650−654.
(13) Martin, J. M.; Sundermann, A. *J. Chem. Phys.* **2001**, *114*, 3408−3420.
(14) Yang, X. *ACS Catal.* **2013**, *3*, 2684−2688.
(15) Custelcean, R.; Jackson, J. E. *Chem. Rev.* **2001**, *101*, 1963−1980.